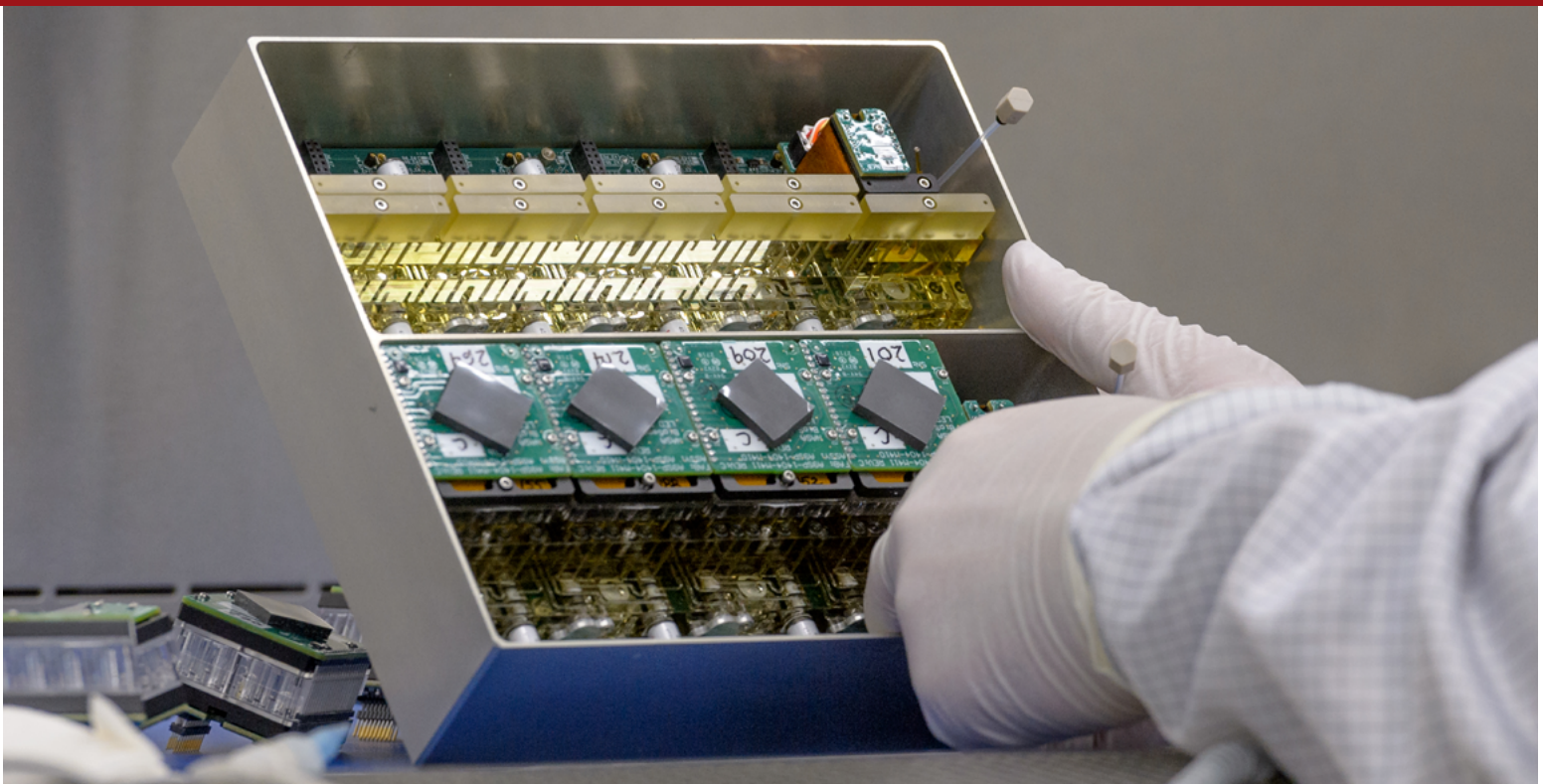


BioSensor Users' Guide





Authors: Matthew Lera, Michael Padgen, Ph.D., and Jessica Lee, Ph.D.

Introduction

The BioSensor is a fully autonomous 3-color LED-based spectrophotometer paired with a fluidics system that supports microbes in liquid culture. Originally developed for the BioSentinel CubeSat mission to study the response of a wild type and mutant strain of yeast to the deep space environment, the BioSensor consists of a series of 16-well, independently plumbed fluidics cards. The cards utilize filters to allow the fluidic system to administer reagents while constraining the microbes in their wells. Heaters on each card incubate to the appropriate growth temperature once the experiment begins. During the active experiment, the LED/detector system measures the transmission of light through each well at three specific wavelengths, similar to a standard benchtop spectrophotometer. The transmission/absorbance kinetics curves for each well are telemetered back to Earth, along with temperature data, for analysis on the ground. The BioSensor is being upgraded from its original CubeSat free-flyer interface to be a secondary payload on lunar landers, Gateway, and other BLEO applications, while maintaining the same functionality and science utility for future experiments.

Planned and Past Research

CubeSat Heritage

NASA Ames Research Center has a rich pedigree of developing and executing biological CubeSat missions over the past two decades in support of Space Biology and Astrobiology experiments investigating various organisms' response to microgravity and radiation, or the response to an antimicrobial agent in the space environment (Massaro Tieze *et al.*, 2020). To date, this pedigree includes GeneSat-1 (Ricco *et al.*, 2007), O/OREOS - Organism/Organic Exposure to Orbital Stresses (Nicholson *et al.*, 2011; Nicholson and Ricco, 2020), PharmaSat (Parra *et al.*, 2008; Ricco *et al.*, 2011), SporeSat (Park *et al.*, 2017), and E. coli AntiMicrobial Satellite (EcAMSat) (Matin *et al.*, 2017; Padgen *et al.*, 2020a), all of which were conducted in Low Earth Orbit (LEO). These missions involved maintaining organisms in stasis in fluidic cards prior to launch. Once launched and inserted in a stable orbit, in most cases a fluidic system administered growth media to the cells in stasis to initiate growth in space. In the case of PharmaSat and EcAMSat, the cells were also challenged with an antifungal or antimicrobial agent. Due to the nature of SmallSats, the experiments in all cases were completely autonomous with little commanding required from the ground. The data were telemetered to the ground via radio for subsequent analysis.

BioSentinel

BioSentinel will be NASA's first biological CubeSat mission to be conducted in deep space, and will be the inaugural mission of the BioSensor payload. As part of the upcoming Artemis-1 launch on NASA's Space Launch System, BioSentinel will be the only CubeSat of thirteen secondary CubeSat payloads to be deployed in transit to the moon. The goal of the BioSentinel mission is to explore the effects that deep space ionizing radiation has on living organisms, using *Saccharomyces cerevisiae* as a model. *S. cerevisiae* is a standard eukaryotic model organism chosen for its translatability to mammalian systems. It also has significant flight heritage (Padgen *et al.*, 2021) particularly in CubeSats, is an ideal genetic model, and can be preserved by drying. This last point is important for deep space missions since the turnover time from delivery of payload to rocket integrator for launch is typically 6-12 months, significantly longer than space biology researchers are accustomed to on ISS missions (hours to weeks) or CubeSat missions (weeks to a few months).

For the BioSentinel mission, yeast cells are initially desiccated inside a series of microfluidic cards, which are activated at various timepoints throughout the duration of the mission. Desiccation is a departure from previous SmallSat hardware that instead had cells in buffer or water prior to experiment initiation. When the BioSentinel experiment is to begin, the system administers synthetic complete (SC) growth medium and alamarBlue™ to revive the desiccated cells and initiate the experiment. The system then measures absorbance of the rehydrated cultures over time and telemeters the data back to Earth. The absorbance curves at three distinct wavelengths allow for tracking the growth and the metabolic activity of the organisms in each well (Santa Maria *et al.*, 2020). Throughout the mission, the incident radiation is also measured with an onboard radiation spectrometer allowing for correlation of growth and metabolic activity with radiation data. The BioSentinel mission also has an identical payload on ISS to serve as a LEO control, and a third identical payload on the Earth to serve as a ground control (Ricco *et al.*, 2020). Data from the BLEO CubeSat, ISS LEO-control, and their respective ground controls are compared to explore the incidence and repair efficiency of radiation-induced DSBs in the contrasting radiation and microgravity environments.

LEIA

The Lunar Exploration Instrument for space biology Applications (LEIA) mission will also use the BioSensor payload hardware originally designed for the BioSentinel mission, but instead is planned to be a secondary payload on a Commercial Lunar Payload Services (CLPS) lander. To convert the free flyer configuration to one compatible with a CLPS lander, the spacecraft will be removed. However, the payload design will be retained, including fluidics, optical, and thermal systems, with very few modifications, if any, to ensure nominal performance on the surface of the moon. The radiation sensor may also be amended to be better suited for the lunar surface environment, which includes significant secondary neutrons produced from the interaction of Galactic Cosmic Radiation (GCR) with the lunar regolith. CLPS providers typically require turnover of secondary payloads 6-9 months prior to launch. With the hardware build and testing required, the Biology for LEIA must remain viable for 12-18 months in a desiccated state to survive the complete duration from sample integration to experiment start on orbit.

The BioSensor Payload

The BioSensor Payload, originally developed for the BioSentinel mission, employs a fluidic system that includes fluidic cards housing the biology, reagent storage bags for storing media and other fluids needed to execute the experiment, and pumps and valves to mix and deliver reagents to the cards throughout the experiment. Additionally, the payload includes heaters on each card to incubate the cells at the desired temperature (23 °C for the BioSentinel mission). The fluidic card incubating at 23 °C shows minimal deviation from the setpoint between wells. There is negligible heat exchange with neighboring fluidic cards that are not being incubated at active growth temperature [Figure 1]. Heaters are also positioned on reagent bags to ensure reagents do not freeze at any point during the mission. The 3-wavelength LED/detector system is positioned above and below each well of the fluidic cards to measure light absorbance (Ricco *et al.*, 2020).

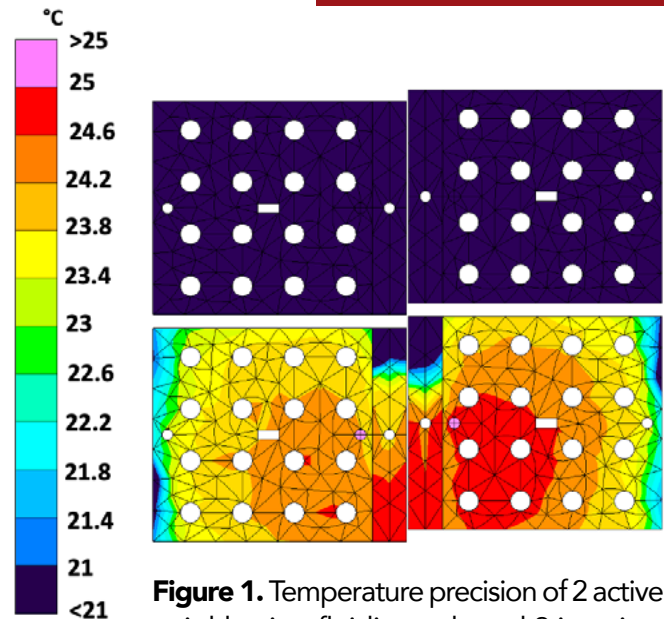


Figure 1. Temperature precision of 2 active neighboring fluidic cards and 2 inactive.

The BioSensor Fluidic System

The payload is comprised of two independent banks. Each bank contains one card manifold that hosts 9 cards, 1 long-pathlength calibration cell, and 1 bubble trap, and 1 bag manifold that contains 1 pump, 1 short pathlength calibration cell, 1 growth medium bag and 1 bag (shared between the two banks) of 10X (stock) alamarBlue [Figure 2]. Bags are composed of fluorinated ethylene propylene (FEP) and total storage capacity is approximately 225 mL between the two banks. For increased flexibility, the number and size of bags may be altered, as each manifold can accommodate up to 3 bags each, not including waste bags. To limit the ambient humidity, the cards and card manifold are stored separately from the fluids. Desiccant and activated carbon cloth are installed in the card box to help promote biocompatibility (Padgen *et al.*, 2021).

At each card position, there is a desiccant chamber that remains in vapor contact with the interior of the card to keep the cells as dry as possible until filling of the wells with fluid. Check valves on the inlet and outlet side of the card constrain the volume of air exposed to the desiccant. Hydrophobic

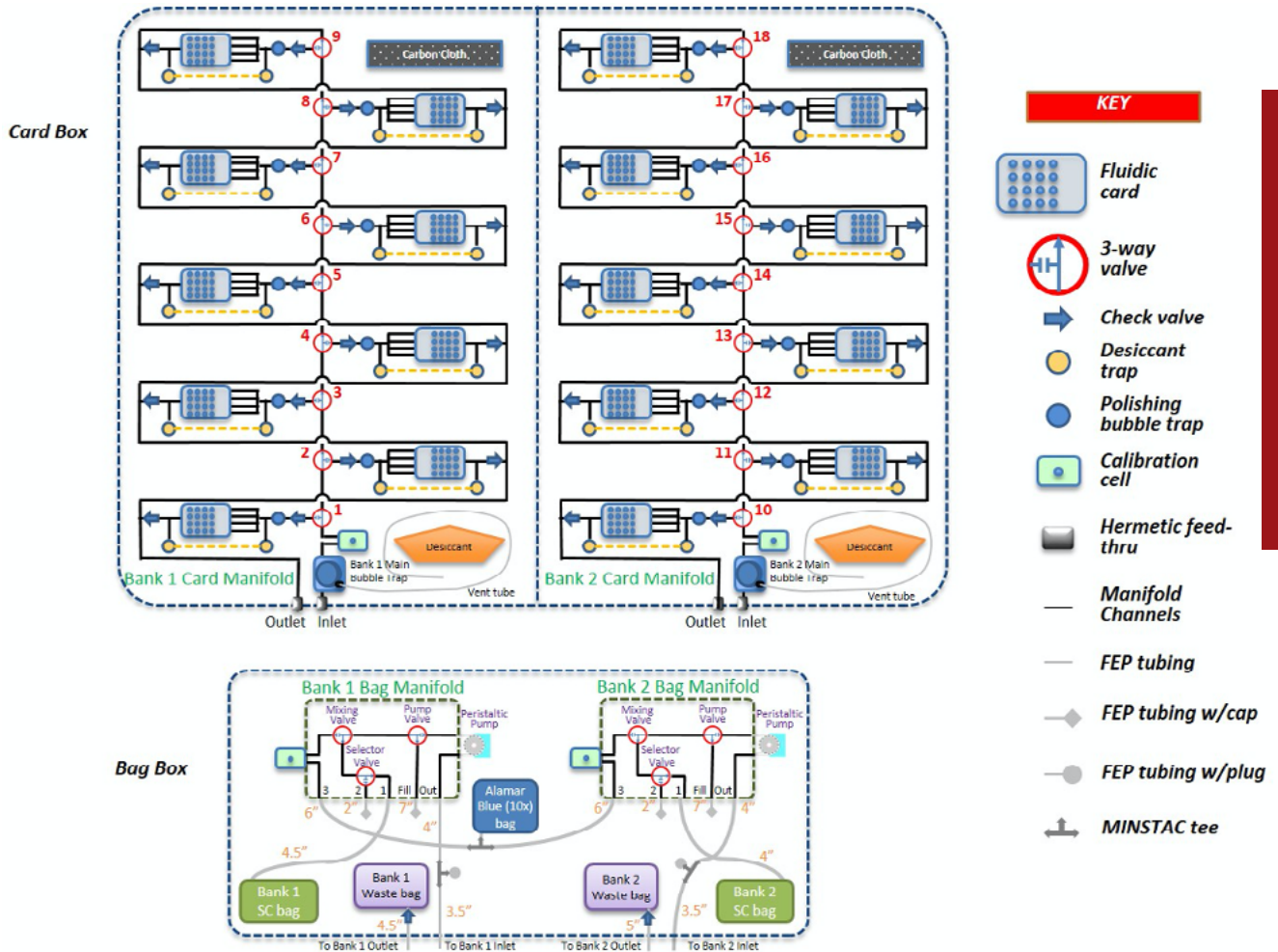


Figure 2. Fluidics schematic

filters separate the desiccant from the fluid flow path. Each position has a 3-way valve. When off, the fluid passes that position and moves to the next, and eventually out of the manifold. When the valve is activated the fluid is directed to flow toward the card. It will pass through the inlet check valve, a bubble trap, and into the card. Once the card has been filled, the fluid exits the card, passes through another check valve and empties into the waste line. Only one card can be filled at a time.

Each bag manifold contains 3 ports for fluidic bags, one port for filling the bags, and one “out” port that connects to the respective inlet port on the card box. One bag port is connected to a short pathlength calibration cell, which can be used to monitor the absorbance of a concentrated dye over the course of the experiment. Dilution can be achieved by toggling valves on and off. Prior to the experiment, all channels and tubing downstream of the pump valve are maintained as dry. Waste bags for each bank are connected to the respective port on the card box.

The BioSensor Fluidic Card

The fluidic card is a completely autoclavable design of primarily polycarbonate material, which contains 16 microfluidic wells of 100 μ L volume each [Figure 3]. The BioSentinel payload configuration accommodates 18 independent fluidic cards, but this number may be reduced for future shorter-duration missions with different power and thermal budgets. The wells of each card are launched dry with desiccated cells typically adhered to the walls of the wells. Once on orbit the fluidic system administers reagents to the cards to fill the wells and initiate the experiment. Sandwiched around each card is a filter membrane, μ channel layer, and impermeable cover that collectively allow for the administration of fluids to each well [Figure 4]. Outside the fluidic components of the card there are heaters and thermal spreaders to achieve a uniform incubation temperature. The card stack is sandwiched by the LED optical source PCB on one side and the optical detection PCB on the other (Ricco *et al.*, 2020).

The BioSensor Optical System

The payload offers absorption values for each well via 3 LEDs positioned above each well and detector chips positioned on the opposite side [Figure 4]. The LEDs provide illumination (in the BioSentinel configuration, wavelengths are 570, 630, and 850 nm, sequentially); absorbances are calculated from the output of a dedicated intensity-to-frequency light sensor (ams/TAOS) at each well. The optical system has no moving parts.

The Optical System design has been used in previous missions, and is used in the BioSentinel Mission to detect metabolic activity by measuring the color change kinetics of the redox reporter dye alamarBlue. Example data can be seen in Figure 5, which shows the absorbance at 570 (green), 630 (red), and 850 nm (NIR, gray) for one well with wild-type (WT) yeast cells (solid lines) and one well with mutant yeast cells (dotted lines). The drop in the red absorbance (~20 and ~48h for wild type and mutant respectively)

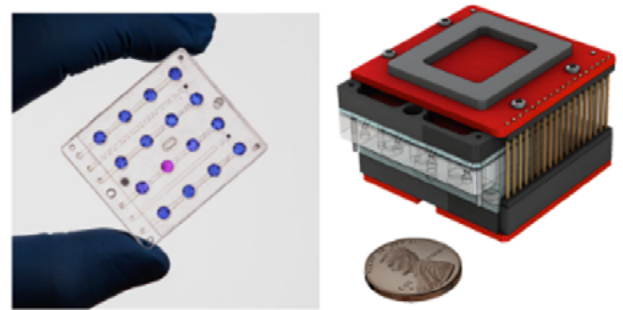
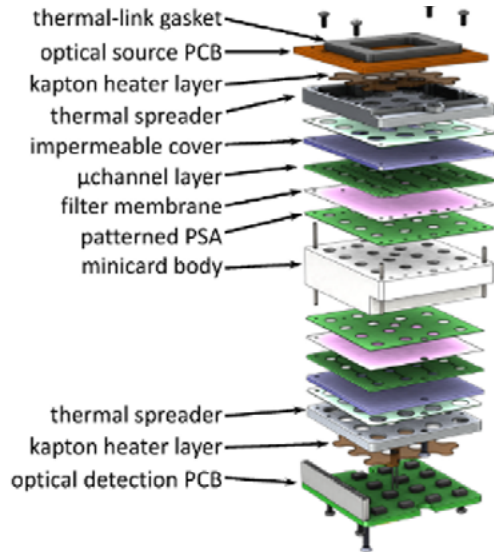


Figure 3. Exploded (top) and assembled (lower right) views of the microfluidic minicard with integral thermal control and optical measurement components. Bottom left: photo of a fluidic minicard; 15 microwells contain aB and one contains the same dye that has turned pink (has been biochemically reduced) due to yeast metabolic activity.

results from the reduction of the alamarBlue dye, which changes in color from blue to pink upon reaction with byproducts of yeast metabolism. The increase in the green absorbance at the same time is due to the relatively greater absorbance of the pink form at 570nm. The green absorbance then drops as aB is further reduced to a colorless form. The wavelengths of the three LEDs are optimized to the alamarBlue assay. The 570nm and 630nm LEDs were chosen to measure the gradual color change of the alamarBlue, showing the transition from blue to pink to clear. The third LED at 850nm was chosen to measure the optical density at a wavelength transparent to the alamarBlue color change. If optical density were measured at the more standard 600nm, the data would be skewed by alamarBlue and would vary as the reagent is reduced. LEDs can be swapped for different wavelengths to accommodate other colorimetric assays, but a feasibility assessment must be conducted on a case-by-case basis to ensure the selected LED intensity is sufficient for the specific assay, and the impacts to overall payload power and thermal systems are compatible. Should another colorimetric assay be selected for future missions, the reagents used must also be shelf stable without requiring refrigeration (Ricco *et al.*, 2020, Padgen *et al.*, 2021).

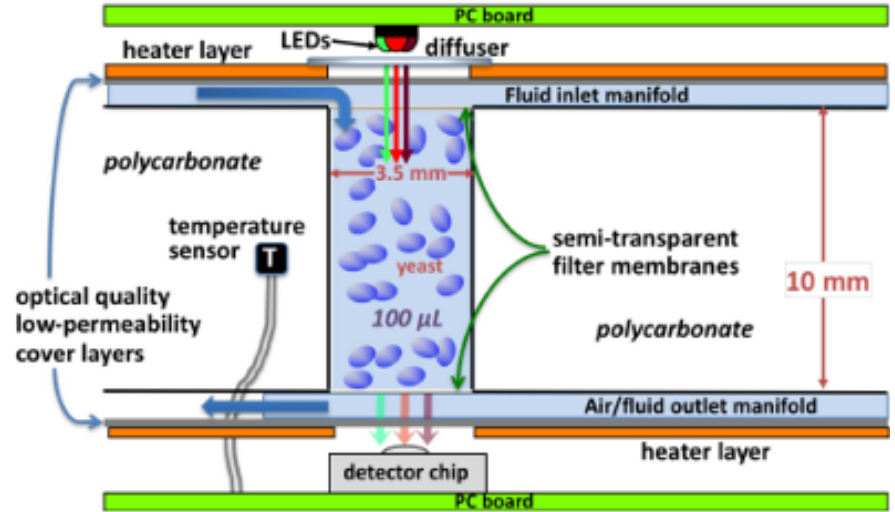


Figure 4. Cross section of single well of polycarbonate fluidic card. 3-wavelength LED sits above each well with a detector on the opposite side to measure light absorbance. 100µL volume (launched dry) is wetted out via the fluid inlet manifold. Cells are constrained to the wells using semi-transparent filter membranes. Heater layers are above and below the cards to provide incubation temperature.

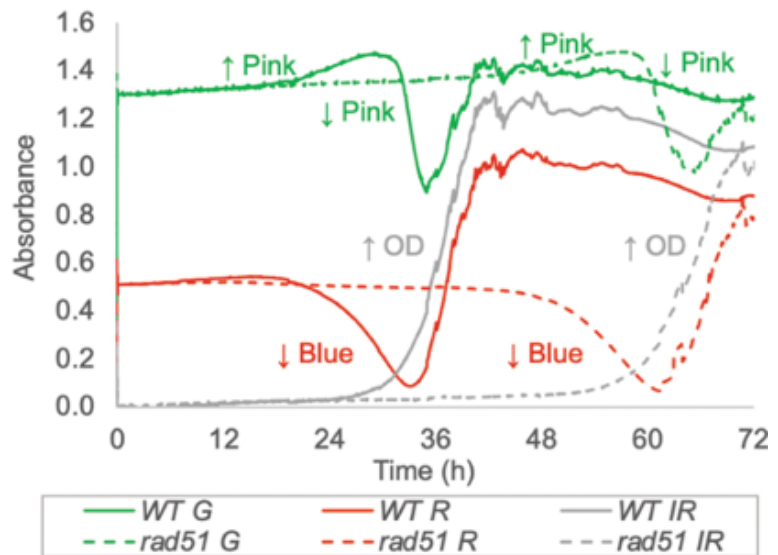


Figure 5. Example data produced by BioSensor Optical Sensor showing the reduction of alamarBlue from blue to pink over time. A third wavelength (gray lines) shows the optical density of the well as the culture is actively growing.

Supplemental Hardware

In order to facilitate iterative lab testing, a Well Plate Adapter was created [Figure 6]. The polycarbonate adapter accommodates two fluidic cards, and features embedded fluidic channels for administering reagents. Fluidic connections to the manifold are made with FEP tubing with .062 MINSTAC fittings. This tubing can be connected via adapters to standard silicone tubing to assemble a surrogate manifold (see branched tubing diagram below). The entire set up (silicone tubing, FEP tubing, fittings and well plate adapter) can be autoclaved. Coupled with a benchtop microfluidic pump, this rig does not require the full Biosensor system, and therefore can support more rapid laboratory testing, making it appropriate for biocompatibility, proof-of-concept, and other experiments. The Well Plate Adapter allows microfluidic cards to be read on a standard multiwell plate reader without the need to disconnect the fluidics, as the wells of fluidic cards mounted in the adapter are designed to align with locations of wells on a standard 96-well plate. This makes it possible to conduct experiments and monitor optical density or absorbance during the course of growth in the fluidic cards, for periods as long as several days. Procedures, parts lists for connecting hardware, and training on loading cards, building the manifold, and integrating the Well Plate Adapter are available.

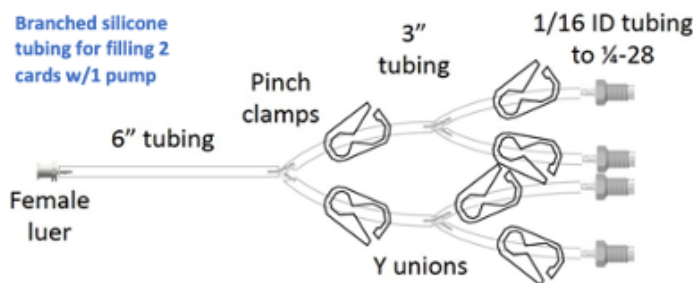


Figure 6. Well Plate Adapter (right) with incorporated fluidic cards. Embedded fluidic channels filled with green dye for visualization. Surrogate manifold schematic (left) featuring standard lab fluidic components.

Lessons Learned from Previous Missions

Over the past several missions, NASA Ames' research teams have collected invaluable experience and lessons learned designing hardware and science experiments for CubeSat missions. These lessons should be considered by any user of the BioSensor as they develop their experiment and testing strategy for future missions.

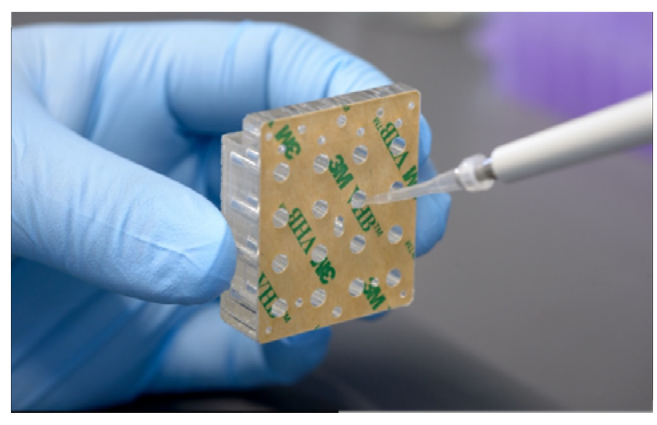
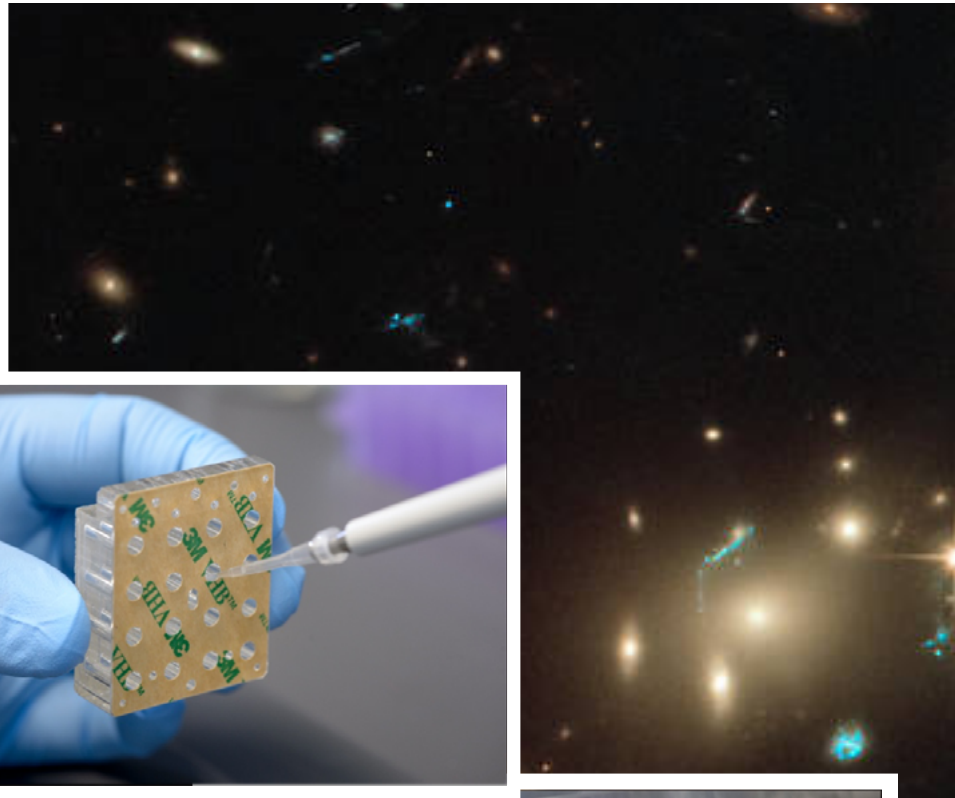
Incorporate Sample Redundancy – Since some wells may be lost in the process of executing the experiment, often during the initial card fill steps, sample redundancy should be incorporated into the experiment design to ensure these small losses can be tolerated. >95% of wells fill, but 1-2 wells per card can have incomplete filling. The presence of bubbles interferes with optical measurements, making interpretation of the results of that well difficult. Sufficient well redundancy ($n > 3$) is required. For example, the BioSentinel mission uses 7 WT and 8 mutant strain wells per card and runs 2 cards simultaneously so each experiment time point has 14 WT and 16 mutant wells.

Include No-cell Reference Wells – This will allow for data normalization and correct for optical drift. Drift in the optical measurements has been observed in this system. While not required, it may be advisable to leave one well per card with no cells, in which the metabolic dye will not be reduced over the course of the experiment. This will provide a consistent baseline measurement from which drift correction terms can be calculated.

Conduct Stasis Viability Testing – The time between sample integration and experiment start is significant. This prevents full-duration iterative testing from being completed within the hardware itself. Therefore, desiccation methods must be tested independently, and the protocol used must confer high confidence that cell viability will be maintained long-term. BioSentinel optimized the procedure extensively with yielded a protocol for drying in the presence of a concentration of trehalose ideal for the cell type. This research is published in (Santa Maria *et al.*, 2020) Ultimately, the protocol chosen must prove effective for the cell type used.

Take Storage Conditions Into Account In Selection and Pre-Treatment of Culture Media – Reagents used must be compatible with the fluidic system. Any precipitates that may form over time may clog filters, pumps, or valves of the fluidic system. Therefore, pre-precipitating and/or filtering should be considered for any reagent with such a risk. Since refrigeration is not possible after integration, any reagent chosen must be stable at room temperature long-term as well.

Oxygen may be a limiting substrate in duration of experiment – The oxygen available to cells while the experiment is active is limited to that which is dissolved in the media itself. Therefore, during the growth phase the cells used will likely exhaust all available oxygen and enter anaerobic growth. This should be considered when designing the experiment. If significant nutrient source is provided resulting in an extended anaerobic growth phase, CO₂ production may result in the formation of bubbles which will obscure the optical data.



References

Massaro Tieze, S., Liddell, L.C., Santa Maria, S.R., Bhattacharya, S. (2021) BioSentinel: A biological cubesat for deep space exploration. *Astrobiology* 20, doi:10.1089/ast.2019.2068.

Matin, A.C., Wang, J.H., Keyhan, M., Singh, R., Benoit, M., Parra, M.P., Padgen, M.R., Ricco, A.J., Chin, M., Friedericks, C.R., Chinn, T.N., Cohen, A., Henschke, M.B., Snyder, T.V., Lera, M.P., Ross, S.S., Mayberry, C.M., Choi, S., Wu, D.T., Tan, M.X., Boone, T.D., Beasley, C.C., Piccini, M.E., and Spremo, S.M. (2017) Payload hardware and experimental protocol development to enable future testing of the effect of space microgravity on the resistance to gentamicin of uropathogenic *Escherichia coli* and its sigma S-deficient mutant. *Life Sci Space Res* 15:1–10.

Nicholson, W.L., Ricco, A.J., Agasid, E., Beasley, C., Diaz-Aguado, M., Ehrenfreund, P., Friedericks, C., Ghassemieh, S., Henschke, M., Hines, J.W., Kitts, C., Luzzi, E., Ly, D., Mai, N., Mancinelli, R., McIntyre, M., Minelli, G., Neumann, M., Parra, M., Piccini, M., Rasay, R., Ricks, R., Santos, O., Schooley, A., Squires, D., Timucin, L., Yost, B., and Young, A. (2011) The O/OREOS mission: first science data from the Space Environment Survivability of Living Organisms (SESLO) payload. *Astrobiology* 11:951–958.

Nicholson, W.L., and Ricco, A.J. (2020). Nanosatellites for biology in space: in situ measurement of *Bacillus subtilis* spore germination and growth after 6 months in low Earth orbit on the O/OREOS Mission. *Life* 10:1–14.

Padgen, M.R., Lera, M.P., Parra, M.P., Ricco, A.J., Chin, M., Chinn, T.N., Cohen, A., Friedericks, C.R., Henschke, M.B., Snyder, T.V., Spremo, S.M., Jing-Hung, W., and Matin, A.C. (2020a) EcAMSat spaceflight measurements of the role of sigma S in antibiotic resistance of stationary phase *Escherichia coli* in microgravity. *Life Sci Space Res* 24:18–24.

Padgen, M.R., Liddell, L.C., Bhardwaj, S.R., Gentry, D., Marina, D., Parra, M., Boone, T., Tan, M., Ellingson, L., Rademacher, A., Benton, J., Schooley, A., Mousavi, A., Friedricks, C., Hanel, R.P., Ricco, A., Bhattacharya, S., Santa Maria, S.R. (2021) BioSentinel: A biofluidic nanosatellite monitoring microbial growth and activity in deep space. *Astrobiology* 21, doi:10.1089/ast.2020.2305.

Park, J., Salmi, M.L., Wan Salim, W.W.A., Rademacher, A., Wickizer, B., Schooley, A., Benton, J., Cantero, A., Argote, P.F., Ren, M., Zhang, M., Porterfield, D.M., Ricco, A.J., Roux, S.J., and Rickus, J.L. (2017) An autonomous lab on a chip for space flight calibration of gravity-induced transcellular calcium polarization in single-cell fern spores. *Lab Chip* 17:1095–1103.

Parra, M.P., Ricco, A.J., Yost, B., McGinnis, M.R., and Hines, J.W. (2008). Studying space effects on microorganisms autonomously: GeneSat, PharmaSat, and the future of bionanosatellites. *Gravitational and Space Biology* 21:9–18.

Ricco, A.J., Hines, J.W., Piccini, M., Parra, M., Timucin, L., Barker, V., Storment, C., Friedericks, C., Agasid, E., Beasley, C., Giovangrandi, L., Henschke, M., Kitts, C., Levine, L., Luzzi, E., Ly, D., Mas, I., McIntyre, M., Oswell, D., Rasay, R., Ricks, R., Ronzano, K., Squires, D., Swais, G., Tucker, J., and Yost, B. (2007) Autonomous genetic analysis system to study space effects on microorganisms: results from orbit. In *Proceedings of the 14th International Conference on Solid-State Sensors, Actuators and Microsystems (Transducers '07/Eurosensors XXI)*, IEEE, New York.

Ricco, A.J., Parra, M., Niesel, D., Piccini, M., Ly, D., McGinnis, M., Kudlicki, A., Hines, J.W., Timucin, L., Beasley, C., Ricks, R., McIntyre, M., Friedericks, C., Henschke, M., Leung, R., Diaz-Aguado, M., Kitts, C., Mas, I., Rasay, M., Agasid, E., Luzzi, E., Ronzano, K., Squires, D., and Yost, B. (2011) PharmaSat: drug dose response in microgravity from a free-flying integrated biofluidic/optical culture-and-analysis satellite. *Proc SPIE* 7929.

Ricco, A.J., S., Santa Maria, S.R., Hanel, R.P., Bhattacharya, S. (2020) BioSentinel: A 6U Nanosatellite for deep-space biological science, *IEE A&E Systems Magazine* 35, 6–18, doi:10.1109/MAES.2019.2953760.

Santa Maria, S.R., Marina, D.B., Massaro Tieze, S., Liddell, L.C., Bhattacharya, S. (2021) BioSentinel: Long-term *Saccharomyces cerevisiae* preservation for a deep space biosensor mission. *Astrobiology* 2020, doi:10.1089/ast.2019.2073.

